

# Effect of the staggered impeller on reducing unsteady pressure pulsations of a centrifugal pump

Ning Zhang (✉ [nzhang@ujs.edu.cn](mailto:nzhang@ujs.edu.cn))

Jiangsu University

Junxian Jiang

Jiangsu University

Xiaokai Liu

Jiangsu University

Bo Gao

Jiangsu University

---

## Research Article

**Keywords:** staggered impeller, centrifugal pump, numerical simulation, reduction of pressure pulsation

**Posted Date:** April 5th, 2021

**DOI:** <https://doi.org/10.21203/rs.3.rs-308478/v1>

**License:** © ⓘ This work is licensed under a Creative Commons Attribution 4.0 International License.

[Read Full License](#)

---

# Effect of the staggered impeller on reducing unsteady pressure pulsations of a centrifugal pump

Ning Zhang<sup>1</sup>, Junxian Jiang<sup>1</sup>, Xiaokai Liu<sup>1</sup>, Bo Gao<sup>1</sup>

<sup>1</sup>School of Energy and Power Engineering, Jiangsu University, Zhenjiang, 212013, China

**Abstract:** High pressure pulsations excited by rotor stator interaction is always focused in pumps, especially for its control considering the stable operation. In the current research, a special staggered impeller is proposed to reduce intense pressure pulsations of a centrifugal pump with  $n_s=69$  based on alleviating rotor stator interaction. The numerical simulation method is conducted to illustrate the influence of staggered impeller on the pump performance and pressure pulsations, and three typical flow rates ( $0.8\Phi_N$ - $1.2\Phi_N$ ) are simulated. Results show that the staggered impeller will lead to the pump head increasing, and at the design working condition, the increment reaches about 3% compared with the original impeller. Meanwhile, the pump efficiency is little affected by the staggered impeller, which is almost identical with the original impeller. From comparison of pressure spectra at twenty monitoring points around the impeller outlet, it is validated that the staggered impeller contributes significantly to decreasing pressure pulsations at the concerned working conditions. At the blade passing frequency, the averaged reduction of twenty points reaches 89% by using the staggered impeller at  $1.0\Phi_N$ . The reduction reaches to 90%, 80% at  $0.8\Phi_N$ ,  $1.2\Phi_N$  respectively. Caused by the rib within the staggered impeller, the internal flow field in the blade channel will be affected. Finally, it is concluded that the proposed staggered impeller surely has a significant effect on alleviating intense pressure pulsation of the model pump, which is very promising during the low noise pump design considering its feasibility for manufacturing.

**Keywords:** staggered impeller, centrifugal pump, numerical simulation, reduction of pressure pulsation

## Nomenclature

$Q_d$	Pump capacity, m <sup>3</sup> /h
$H_d$	Design head, m
$n_d$	Design speed, r/min
$n_s$	Specific speed
$\Phi_N$	Flow coefficient
$\Psi_N$	Head coefficient
$Z$	Blade number
$\eta$	Efficiency
$D_1$	Impeller suction diameter, mm
$D_2$	Impeller exit diameter, mm
$D_4$	Volute exit diameter, mm
$b_2$	Impeller exit width, mm
$\phi$	Wrap angle of the blade, °
$u_2$	Peripheral speed at the blade outlet, m/s
$\delta$	Rib width, mm
$\rho$	Water density, m <sup>3</sup> /h
$A$	Pressure value, Pa
$c_p$	Pressure coefficient
$\theta$	Angle of the monitoring point, °
$w$	Relative velocity, m/s
$\Omega_z$	Vorticity magnitude along z direction, 1/s
$y^+$	y plus value
$\Delta t$	CFD time step, s
$f_n$	Rotating frequency, Hz
$f_{BPF}$	Blade passing frequency, Hz

## Introduction

As the general and common machinery, pumps are used in almost all the industrial fields, and the corresponding stable operation are strictly required in special fields, for example the nuclear power plant and petrochemical industry[1,2]. As for the stable and safe working of the pump, it is considered to be associated with the flow induced pressure pulsations, which is mainly originated by the rotor-stator interaction(RSI)[3-4]. So, pressure pulsations are always emphasized and

investigated during the pump design and its operation[5].

For pressure pulsation in centrifugal pumps, two topics are mainly discussed, namely the generating mechanism and the corresponding control. RSI resulted by the impeller periodically sweeping the tongue is the primary factor accounting for high and intense pressure pulsations in centrifugal pumps, which is investigated and validated by many researchers[6,7]. Pressure spectral characteristics at different working conditions were clarified. It was found that pressure signals show periodic characteristic at the design working condition. In pressure spectrum, caused by RSI effect, the discrete peaks at  $f_{BPF}$  (blade passing frequency) and its high harmonics with lower amplitudes could be captured[8,9]. So, the frequency at  $f_{BPF}$  keeps the predominant role in spectrum as manifested by the maximum pressure magnitude when the centrifugal pump works around the nominal flow rate as pointed by Yao et al[10]. At off-design flow rates, pressure pulsation amplitude at  $f_{BPF}$  will be affected[11]. At low flow rate, the flow separation with large scale in the blade channel will lead to the increment of pressure pulsation, and at high work conditions, the stronger interacting effect between the non-uniform fluid and the tongue will also lead to high pressure pulsation. It means that pressure pulsation will be minimized around the design working condition[12].

As for the control of pressure pulsation, the RSI effect is mainly concentrated, and some effective approaches were discussed. Yang et al proved that the rotor-stator gap is crucial for pressure pulsations, and positive effect will be generated by increasing the gap[13]. Posa et al also validated that the large gap will be beneficial for reducing pressure pulsation amplitude by rotating the diffuser blade around the middle chord[14]. Al-Qutub et al discussed the influence of blade V-cut on complex pressure pulsation, and it is validated that the V-cut can reduce pressure pulsations[15]. Recently, many researchers believe that the rotor-stator interaction is determined by the flow distribution at the blade trailing edge (BTE), and by controlling the flow distribution at trailing edge of the impeller, unsteady pressure pulsation energy could be decreased[16]. From such point, Gao et al analyzed the effect of BTE shape on pump performance and unsteady pressure pulsation, and results show that the BTE shape surely affects pressure pulsation energy[17,18]. The reason is due to the changing of flow distribution by modifying the BTE shape, and the flow uniformity could be improved significantly by the reasonable BTE shape.

Based on the published works, unsteady pressure pulsation energy within the centrifugal pump is affected by two factors, and one is the fluid distribution characteristics at the BTE and the other is the corresponding intense interacting effect with the tongue. So, if we can control and reduce the striking effect between the fluid discharged from the BTE and the volute tongue, then pressure pulsation energy could be decreased[19-21]. For the commonly used impeller, when the wrap angles from the shroud to the hub streamlines are identical, fluid discharged from the impeller will hit and interact with the tongue simultaneously[22,23], namely with the same phase. Finally, high pressure pulsations will be excited. It is inferred that if the flow from the shroud to the hub does not interact with the tongue simultaneously, namely the phase difference is generated by some special impeller types, then pressure pulsation may be reduced.

Based on the above analysis and assumption, in the current paper, a special staggered impeller is proposed to reduce pressure pulsations in a centrifugal pump. The impeller is divided into two sections by a rib in the middle plane, and the phase difference will be generated. To investigate effect of the staggered impeller on the pump performance and complex pressure pulsation, the unsteady numerical simulation method was applied, and the corresponding accuracy was validated by the experiment. Emphasis was laid on the resulting influence on pressure pulsations, and twenty monitoring points were placed around the impeller exit to extract pressure signals and to evaluate the positive effect comprehensively. Meanwhile, three typical flow rates were carried out for the staggered impeller, which were compared with the original impeller in detail. Finally, the effect of staggered impeller on the performance and pressure pulsation will be clarified. The obtained results in the present paper will provide a direction to control pressure pulsation energy in centrifugal pump considering its strong maneuverability.

## 1. Numerical setup

### 1.1 Model pump for investigation

In this study, the model pump with two dimensional blade is used for investigation. Some basic parameters of the model pump are presented in table.1. During the pump design, the original impeller includes six blades. For the proposed staggered impeller, it could be divided into two parts by a rib in the middle of the impeller, namely the front blade and the back blade. The distance between the front and the back blade is  $\delta=1\text{mm}$ . The intersection angle between the front and back blades is  $30^\circ$  as shown in fig.1. It means that for the original blade, it will be separated into two parts by the rib, then the back blade will be rotated by  $30^\circ$ . Finally, the staggered impeller will be formed, and the shape of the staggered impeller is the same with the original impeller. The phase difference will be generated between the front blade and the back blade when the fluid interacts with the tongue. The active outlet width of the staggered blade equals to the original impeller, namely the cross section area of the staggered impeller does not change. Finally, the influence of the rib on the flow capacity could be eliminated.

### 1.2 Mesh generation

During the numerical simulation, the computational domain is established, and it contains four parts, the staggered impeller, volute, inlet duct and outlet duct. Fig.2 presents the used computational domain for the numerical calculation. As

for the model pump, the structured mesh grids are created by the ICEM software. The boundary layer near the solid wall is more easily to control and generate from comparison with the unstructured grids. Fig.3 shows the generated mesh grids of the staggered impeller. Obviously, the grid around the solid wall of the blade is encrypted to guarantee the  $y^+$  value to be in the reasonable range[24,25]. For the impeller, the height of first layer grid is set as 0.1mm, and the growth ratio of the mesh grid is 1.1. Finally, 5 million structured grids are created for the impeller and 4 million for the volute, and about 11 million grids are generated for the calculated computational domain. Fig.4 shows the  $y^+$  distribution at the blade surface. At the design working condition, the predicted  $y^+$  value on the blade wall from the steady result reaches 5. It is believed that with the current mesh grids, the typical flow structures could be resolved precisely.

Table.1 Parameters used for the current pump

Parameters	Value
Pump flow rate $Q_d$	55 m <sup>3</sup> /h
Pump head $H_d$	20 m
Rotation speed $n_d$	1450 r/min
Specific speed $n_s = 3.65n_d \sqrt{Q_d} / H_d^{0.75}$	69
Blade number $Z$	6
Impeller suction diameter $D_1$	80 mm
Impeller exit diameter $D_2$	260 mm
Volute exit diameter $D_4$	80 mm
Outlet width of the original impeller $b_2$	17 mm
Blade exit angle $\beta_2$	30°
Blade wrap angle $\phi$	115°
Outlet width of the staggered impeller $b_2$	18mm
Rib width $\delta$	1mm
Peripheral speed at the impeller exit $u_2$	19.7 m/s

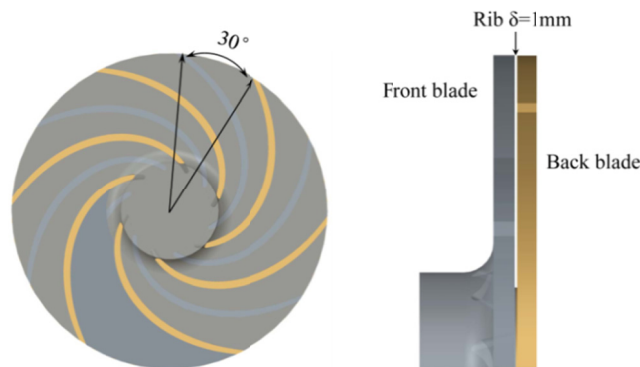


Fig.1 Structure of the staggered impeller

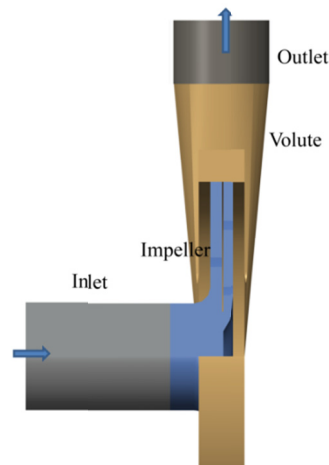


Fig.2 Computational domain established for calculation

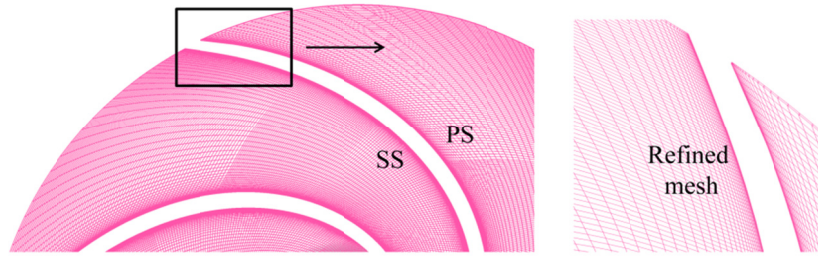


Fig.3 Mesh grids of the used staggered blade

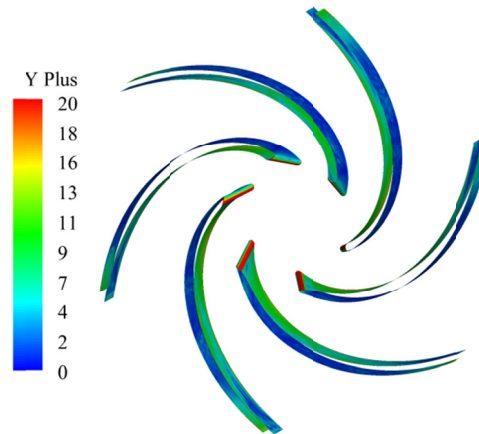


Fig.4 Values of  $y^+$  on the blade surface at the design flow rate

### 1.3 Numerical method

During the steady numerical simulation, the SST  $k-\omega$  turbulent model was conducted to obtain the pump performance. The inlet and outlet ducts are prolonged to at least three times of the pump suction diameter to achieve the stable inflow and outflow conditions. Meanwhile, at the inlet, the velocity boundary condition is given, which is calculated from the pump flow rate. At the pump outlet, the pressure outlet condition with a constant value  $p=1.0 \times 10^5 \text{ Pa}$  is used. To deal with the relative motion between the volute and the impeller, the moving reference frame approach is used. During the simulation, all solid surfaces of the computational domain were regarded as the non-slip wall. To couple the data transfer between two computational domains, the interface is applied. The least square cell method was used to solve the gradient spatial discretization, and first upwind scheme is conducted to dispose the spatial discretization during simulation. Meanwhile, for the coupling of the pressure and velocity, the SIMPLE scheme is used during the calculation. The residual value  $3.0 \times 10^{-5}$  is set as the convergent standard, and the pump performance keeps unchanged when the residual reaches the set value.

To obtain influence of the staggered impeller on unsteady pressure pulsations at various working conditions, the transient calculation is conducted by the LES method. The Smagorinsky-Lilly (SM) model is adopted to close the

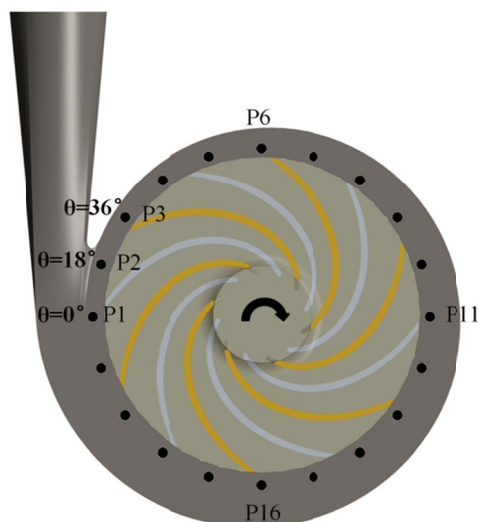


Fig.5 Twenty points around the impeller exit during calculation

governing equation, and the corresponding accuracy is validated by Poas et al[26]. As for the governing equation of LES approach, it can be found in the published research[26]. For the unsteady calculation of the model pump, the relative motion between the volute and impeller is solved by the moving mesh approach. The time step is the most crucial parameter during unsteady simulation, which is set as  $\Delta t=1.15 \times 10^{-4} \text{s}$ [27,28]. Namely, the pressure value and flow field will be analyzed and obtained at every impeller rotating degree. As for the LES method, the bounded central differencing method is applied to treat the momentum discretization. During calculation, the maximum 60 iterations are set for one time step to ensure the simulation is fully converged. To achieve influence of the staggered impeller on unsteady pressure pulsations of the model pump, twenty points from P1 to P20 are placed around the impeller exit to obtain unsteady pressure signals as presented in fig.5. The start angle at point P1 is defined as zero, which increases with  $18^\circ$  for every monitoring point. During calculation, more than 30 impeller cycles are simulated to gain the periodic pressure signals. Finally, pressure signals in the last ten impeller revolutions are used for the FFT processing to analyze pressure spectral characteristics at various working conditions.

## 2. Results and discussions

### 2.1 Comparison of pump performance

The following equations are used to obtain the non-dimensional pump parameters[29,30].

$$\Phi_N = \frac{Q_d}{u_2 R_2^2} \quad (1)$$

$$\Psi_N = \frac{gH_d}{u_2^2} \quad (2)$$

Here, water density  $\rho$  is  $1000 \text{kg/m}^3$ .

Pump performance comparison between the original and staggered impellers is first shown in fig.6. The pump performance is predicted by SST  $k-\omega$  turbulent model. Meanwhile, the calculation uncertainty is validated by the experimental data of the original impeller[17]. For the general pump, it will operate around the design working condition, so in the current research, pump performance within  $0.6-1.2\Phi_N$  is concerned. From comparison, it is observed that the original pump head coincides well with the experimental data. At  $1.0\Phi_N$ , the numerical error reaches about 1.3%. When the flow rate deviates to  $0.8$  and  $1.2\Phi_N$ , the numerical error is lower than 4%. It is inferred that the fluid leaking from the front wear ring is the main reason accounting for the calculation error, which is not considered during the calculation as seen in fig.2. From comparison between the original and staggered pumps, it is evident that the staggered impeller contributes to the improvement of pump performance. For the model pump head under the design working condition, the improvement is about 3%. At off-design flow rates  $0.8\Phi_N$  and  $1.2\Phi_N$ , increments are 2.3% and 3.6% respectively. As observed from the pump efficiency, it is found that the effect of staggered impeller on the pump efficiency is not significant. The difference is lower than 1% at various flow rates. Finally, by applying the staggered blade, significant effect on the pump performance will be generated, especially for the pump head.

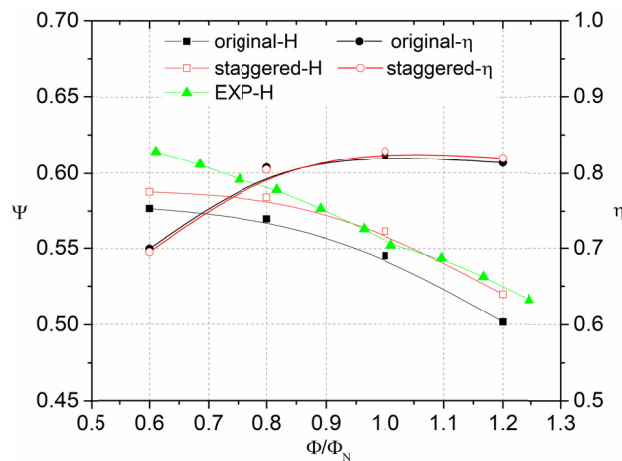


Fig.6 Pump performance comparison

### 2.2 Effect of the staggered impeller on unsteady pressure pulsations

Pressure coefficient is used for investigation as calculated in Eq.(3).

$$c_p = \frac{A}{0.5\rho u_2^2} \quad (3)$$

Where A is pressure value.

The main objective to develop the staggered impeller is to reduce pressure pulsations of the centrifugal pump. To analyze the resulting influence of the staggered impeller on unsteady pressure pulsation, fig.7 shows pressure pulsation signals at four different monitoring points, namely  $\theta=0^\circ$ ,  $\theta=36^\circ$ ,  $\theta=72^\circ$ ,  $\theta=108^\circ$  for the pump under the design working condition. Pressure signals are dimensionless disposed by Eq.3. The rotating cycle is  $T=0.0414s$ , and the corresponding rotating speed is  $n=1450r/min$  of the model pump. From fig.7, it is noted that for the original pump, pressure signals pulsate intensively. Resulting from the rotor-stator interaction, alternative peaks will generate within one impeller rotating cycle, which are determined by the blade number. From the comparison between the original impeller and staggered impeller, we can find that pressure amplitude is decreased significantly. Especially at points  $\theta=36^\circ$  and  $\theta=108^\circ$ , the reduction reaches about 50%. It means that the staggered impeller contributes to decreasing pressure pulsation in the centrifugal pump obviously. The reason is associated with RSI effect. It is well accepted that pressure pulsation in the centrifugal pump is mainly generated by RSI effect, which is originated from the flow striking the volute tongue. As for the staggered blade, due to the phase difference, the fluid discharged from the front and back blade channels will not interact with the tongue simultaneously when the blade sweeps the tongue, and the corresponding interacting effect is much stronger for the original impeller. So, the interaction effect will be decreased significantly by using the staggered impeller, which accounts for the decrease of pressure pulsation when the special staggered impeller is applied.

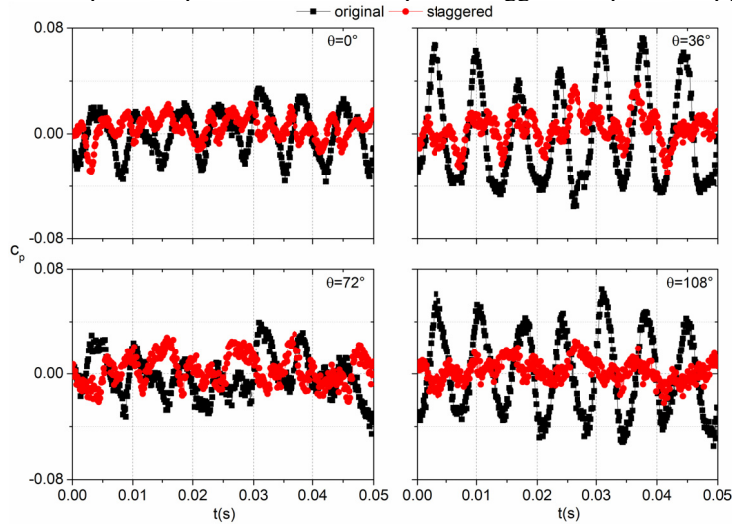


Fig.7 Pressure signals at four points of the original and staggered impellers

To gain the influence of staggered impeller on spectral characteristics, pressure pulsation signals are transformed using the FFT method. Fig.8 shows pressure spectra of four points from  $\theta=0^\circ$  to  $\theta=108^\circ$ . The impeller rotating frequency is  $f_n=24.2Hz$ , so the resulting blade passing frequency will be  $f_{BPF}=145Hz$  for the original impeller with blade number  $Z=6$ . From the spectrum of the original impeller, the prominent peaks at  $f_{BPF}$  and  $2f_{BPF}$  dominate the spectrum under the design

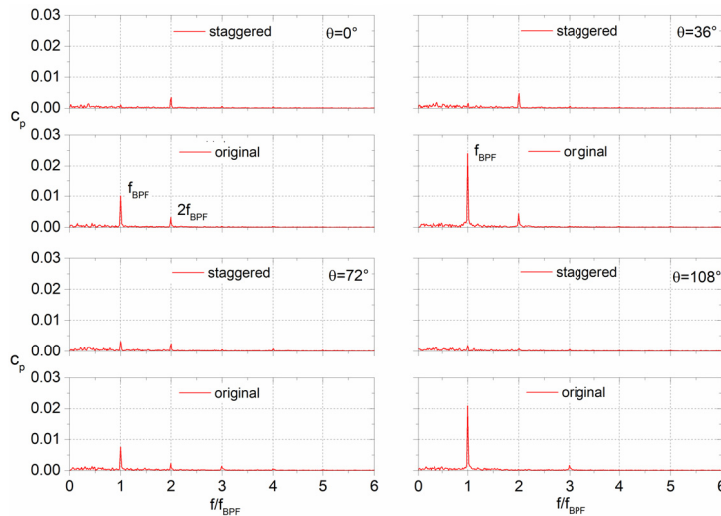


Fig. 8 Pressure spectra at four points from  $\theta=0^\circ$  to  $\theta=108^\circ$  of the original and staggered impellers

working condition. For the staggered impeller, similar phenomenon is observed, namely, the peaks at  $f_{BPF}$  and  $2f_{BPF}$  are generated. From comparison of pressure spectrum, it is validated that at  $1.0\Phi_N$ , pressure amplitude at the blade passing frequency is obviously decreased at all the concerned monitoring points. For points  $\theta=0^\circ$  to  $\theta=108^\circ$ , the final reductions are 89%, 94%, 57% and 94% respectively. Meanwhile, pressure amplitudes of the original and staggered impellers are nearly identical at  $2f_{BPF}$ . Finally, it is proved that the special designed staggered impeller has a distinct effect on decreasing pressure pulsation of the current model pump. The averaged reduction of the four points is about 80%. Meanwhile the component at  $2f_{BPF}$  is almost unaffected. The obtained results coincide with the assumption to reduce rotor stator interaction by proposing the staggered blade.

From fig.7 and fig.8, it is concluded that for the four points, pressure pulsation amplitudes are decreased obviously under the design working condition. To analyze the influence of staggered impeller on the other monitoring points, fig.9 shows comparison of pressure pulsation amplitudes at  $f_{BPF}$  and  $2f_{BPF}$  for the concerned twenty points. For the original pump, due to the intense rotor-stator interaction, pressure amplitudes exhibit a modulated pattern, and peaks and valleys alternatively occur. For the staggered impeller, such phenomenon is not obvious, and at different points, pressure amplitudes are almost equal, especially for the points  $\theta>72^\circ$ . As observed at  $f_{BPF}$ , it is evident that when the staggered blade is adopted, pressure amplitudes at all the twenty monitoring points will be reduced obviously. The averaged value of twenty points is  $c_p=0.01384$  for the original impeller and  $c_p=0.001452$  for the staggered impeller. The corresponding decrease is  $\Delta c_p=89\%$  by using the staggered impeller. From fig.9(b), it is found that the staggered impeller has a little effect on the  $2f_{BPF}$ . As for the averaged values, the difference is about 6%. From comparison of all the twenty points around the impeller exit, it is concluded that by introducing the staggered impeller, rotor-stator interaction will be alleviated significantly as manifested by the decrease of pressure amplitude at  $f_{BPF}$ .

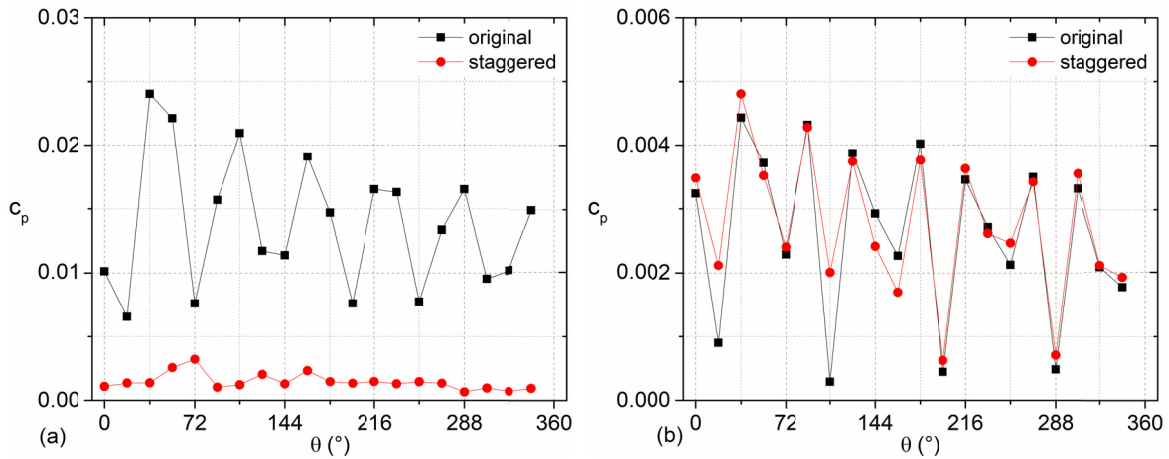


Fig.9 Pressure amplitudes at twenty points under the design working condition, (a) $f_{BPF}$ , (b) $2f_{BPF}$

Centrifugal pumps sometimes work at the off-design flow rates, especially within  $0.8-1.2\Phi_N$ . So, it is also essential to gain the influence of staggered impeller on reducing pressure pulsations when the pump works at off-design flow rates. Fig.10 presents pressure pulsation signals at point  $\theta=36^\circ$  with the pump operating under  $1.2\Phi_N$  and  $0.8\Phi_N$ . From fig.10(a), it is notable that pressure pulsation magnitude of the staggered impeller is also lower than the original impeller, and the reduction reaches about 50%. From fig.10(b), the staggered impeller also contributes to decreasing pressure pulsation at the low working condition. From fig.7 and fig.10, it is concluded that pressure pulsation energy of the pump could also be decreased by the special staggered impeller for the pump working within  $0.8-1.2\Phi_N$ .

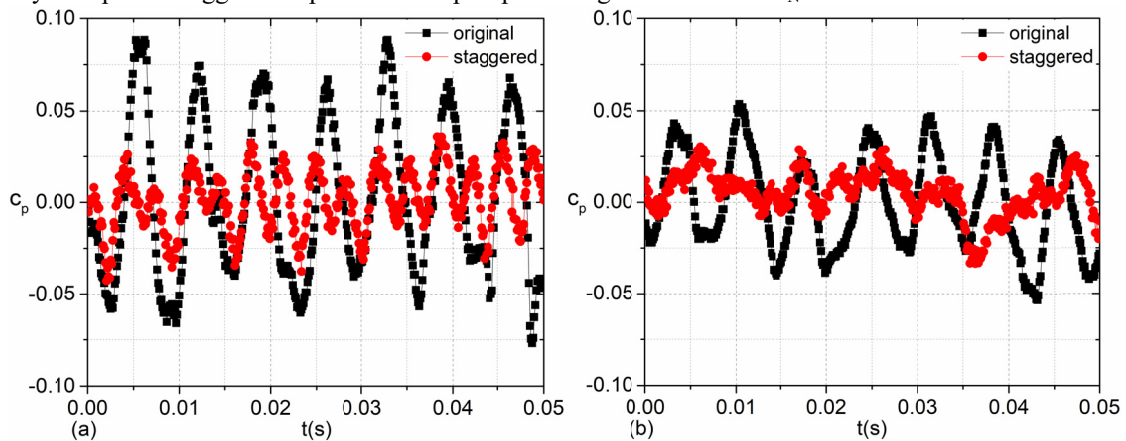


Fig.10 Comparison of pressure signals at  $\theta=36^\circ$ , (a) $1.2\Phi_N$ , (b) $0.8\Phi_N$

Fig.11 shows pressure spectra at the monitoring point  $\theta=36^\circ$  of the staggered and original impellers. From fig.11(a), it is evident that distinct peaks at the blade passing frequency  $f_{BPF}$  and  $2f_{BPF}$  can be identified and captured in pressure spectrum at  $1.2\Phi_N$ . Compared with the original impeller, pressure pulsation amplitude at  $f_{BPF}$  is alleviated significantly, and the reduction is more than 80%. The same phenomenon is also observed when the model pump operates at  $0.8\Phi_N$ . From the above analysis, it is proved that the special proposed staggered impeller contributes to decreasing rotor-stator interaction when the pump operates at various working conditions.

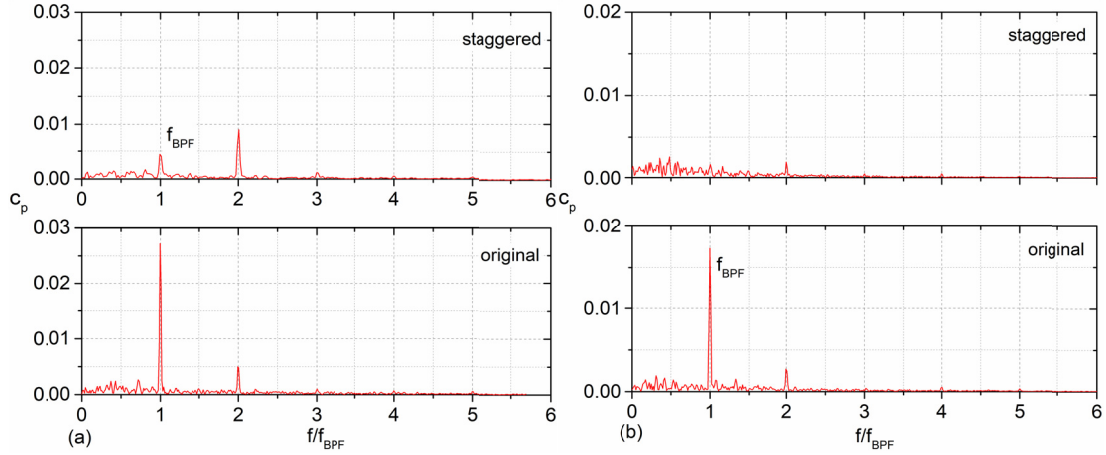


Fig.11 Pressure spectra at  $\theta=36^\circ$  of the staggered and original impellers, (a)  $1.2\Phi_N$ , (b)  $0.8\Phi_N$

To validate the effective influence of staggered impeller on the twenty monitoring points when the pump operates at off-design working conditions, fig.12 shows pressure amplitudes at  $f_{BPF}$  for all the calculated twenty points for the pump operating under  $1.2\Phi_N$  and  $0.8\Phi_N$ . From fig.12(a), the pressure amplitude shows a descending trend at  $1.2\Phi_N$ , which is not obvious in fig.12(b) with the pump operating at  $0.8\Phi_N$  due to the evident flow separation at low working conditions. At  $1.2\Phi_N$ , pressure amplitudes at twenty points are decreased by the staggered impeller. The averaged pressure coefficient is  $c_p=0.0148$  for the original impeller and  $c_p=0.0032$  for the staggered impeller. Finally, the reduction reaches about 80% at  $1.2\Phi_N$ . When the pump operates at  $0.8\Phi_N$ , the averaged pressure coefficients for the original and staggered impellers are  $c_p=0.0113$  and  $c_p=0.00115$  respectively, and the decrement by using the staggered impeller is about 90%. From fig.9 and fig.12, when the staggered impeller is proposed, pressure amplitudes at the concerned twenty points around the impeller exit are reduced significantly, and the averaged reduction is more than 80% for the three calculated flow rates. In the published researches, some approaches were investigated to decrease pressure pulsations in pumps[31,32], however the effect is not as significant as the staggered impeller in the current paper. We believe that the staggered impeller is a very promising technique to alleviate pressure pulsation during the low noise pump design considering the feasibility for its manufacturing.

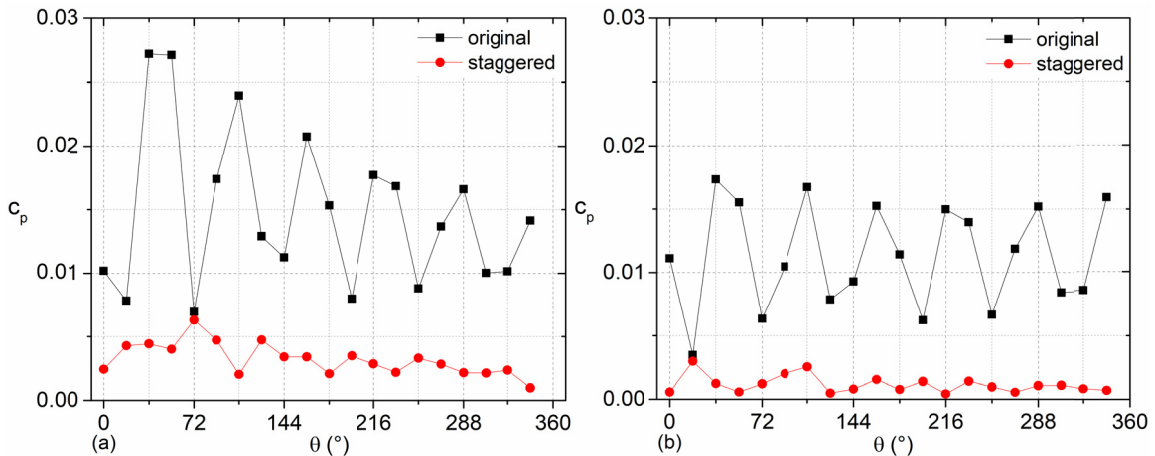


Fig.12 Pressure amplitudes of the twenty points at  $f_{BPF}$ , (a)  $1.2\Phi_N$ , (b)  $0.8\Phi_N$

### 2.3 Typical flow structures within the blade channel

As for the staggered impeller, positive effect will be generated considering the unsteady pressure pulsation. Furthermore, it is also important to obtain the effect of staggered impeller on the internal flow distribution. Here, two cut planes are selected for investigation, namely the planes Section1 and Section2, which locate at the mid-span of the front and back blades as seen in fig.13. As for the original impeller, the same relative positions are also used for comparison.

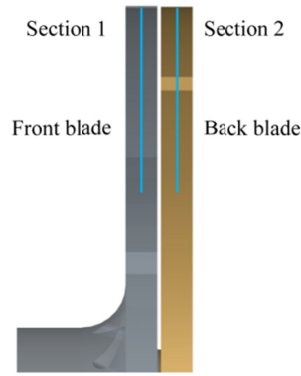


Fig.13 Two cut planes selected for investigation

Fig.14 presents static pressure distributions of the original and staggered impellers on two sections. As observed, pressure distributions are similar, especially on the Section1. From the blade inlet to the outlet, pressure magnitude rises gradually. At the Section2, small difference is observed at the blade inlet, and low pressure area is generated for the staggered impeller. It is inferred that the generating reason is related to the blocking effect of the existing rib on the fluid. Finally, fluid at the blade inlet is accelerated for the staggered blade resulting in the low pressure region, and such phenomenon is also reflected on the internal relative velocity fields in fig.15.

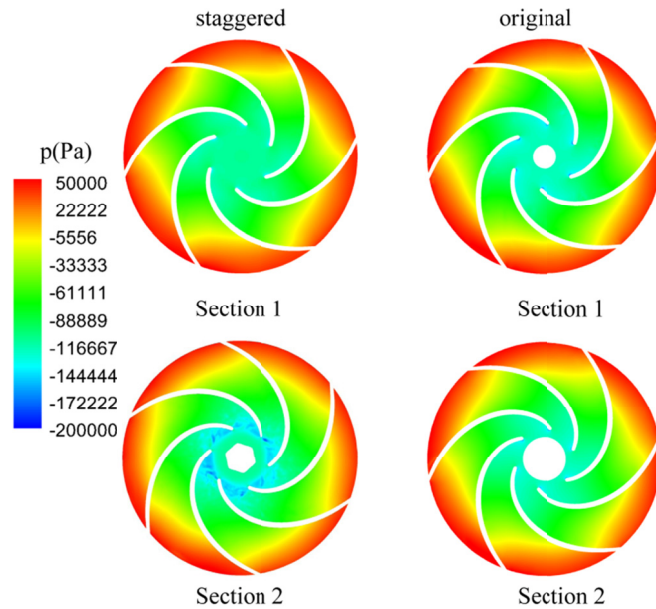


Fig.14 Static pressure distributions on Section1 and Section2

Fig.15 presents the relative velocity distributions on Section1 and Section2 at the design working condition. As noted at Section1, an evident low velocity area is generated around the blade pressure side of the staggered impeller, and the corresponding scale is reduced compared with the original impeller. At the blade suction side, the fluid is accelerated for the staggered impeller as characterized by the high relative velocity. It means that by using the rib, some fluid is forced to move in the front region of the impeller, which will cause the high velocity sheet generating on the blade suction side and minimize the low relative velocity region around the blade pressure side. At Section2, an opposite phenomenon is generated for the staggered impeller, and the low velocity region on the blade pressure side is increased, and it indicates the flow capacity reduction in the back blade channel. From the relative velocity distributions of staggered and original impellers, it is concluded that the rib within the impeller will affect the flow capacities in the front and back blade channels of the impeller even for the low specific speed impeller within two dimensional blade.

To further analyze the influence of staggered impeller on the internal flow structure, vorticity distributions are presented in fig.16 for the two impellers. On Section1, it is observed that high vorticity sheets are developed around the blade surface, especially on the blade suction side for the two impellers. On Section2, significant difference is observed for the staggered impeller. Around the blade leading edge, vortical structures with high vorticity magnitudes are developed, which occupy the blade to blade channel around the leading edge. For such phenomenon, it is caused by the rib in the impeller. Due to the fluid striking the rib, high turbulent flow will be developed. Finally, coherent flow structures will be caused around the blade leading edge. For vorticity distributions towards the blade outlet, no evident difference is observed for the two impellers.

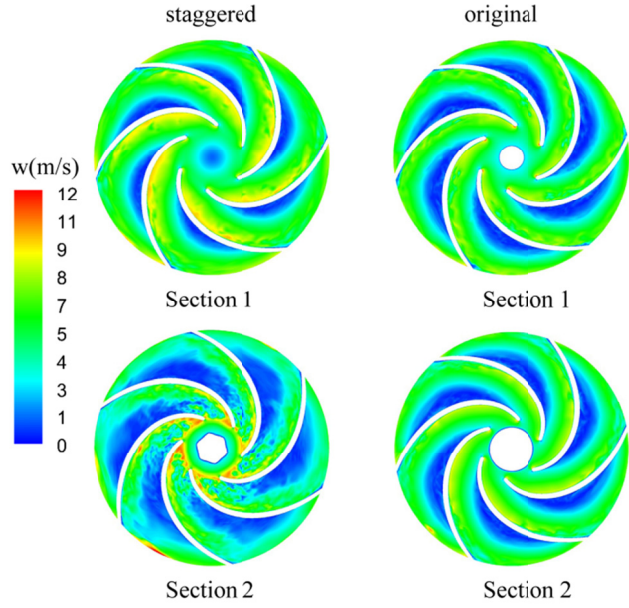


Fig.15 Relative velocity distributions on Section1 and Section2

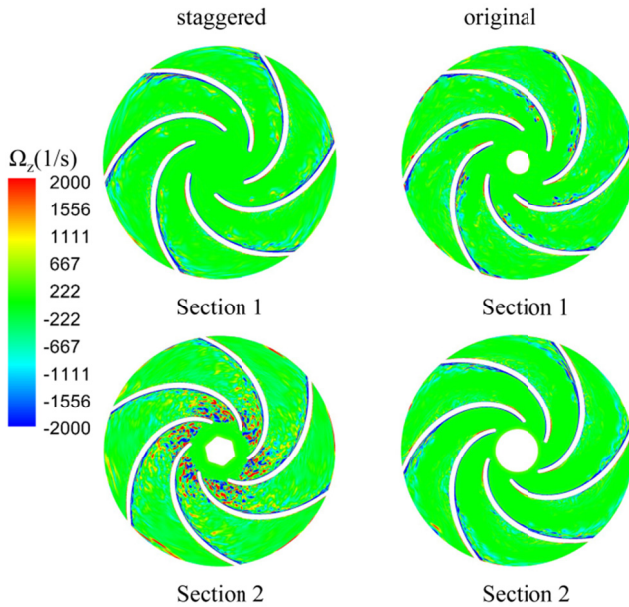


Fig.16 Vorticity distributions on Section1 and Section2 of the two impellers

### 3 Discussion

How to reduce unsteady pressure pulsations in centrifugal pumps is crucial to the pump design to ensure the pump stability during operation[33]. Such topic is discussed by many researchers, and various approaches are proposed to control and reduce the high pressure pulsations[34,35]. As for the unsteady pressure pulsations in pumps, it is mainly originated from the intense rotor-stator interaction. So, pressure pulsation amplitude could be reduced significantly by alleviating the strong RSI effect.

For the RSI effect, it is determined by the interacting effect between the high speed fluid discharged from the impeller and the volute tongue for the single stage centrifugal pump. It means that the striking energy is crucial for the final resulted pressure pulsation amplitude[36-39]. Such opinion is validated in the published paper, and pressure pulsation amplitude will be reduced obviously by increasing the rotor-stator gap. The reason is associated with the reduction of the striking energy of the fluid acting on the tongue. So, it is assumed that by using the staggered impeller, and the phase difference will be generated. Then, the fluid striking energy between the fluid from the blade with the tongue will be alleviated, finally, pressure pulsation amplitude could be decreased significantly.

To validate the above assumption, the staggered impeller is designed and investigated in the present paper. A rib is used to divide the impeller into two parts. The numerical simulation approach is applied to gain the influence of the

staggered impeller on the pump performance and pressure pulsations at three typical working conditions. It is shown that the model pump head will be increased by applying the staggered impeller, meanwhile the pump efficiency changes little. From comparison of pressure amplitude at twenty monitoring points, it is proved that pressure pulsations will be decreased obviously when the special staggered impeller is used. At the design working condition, the averaged reduction reaches 89% at the blade passing frequency.

In the further study, some experiments will be conducted on the staggered impeller, which is an effective approach for the hydraulic design of the low noise pumps in some special fields. Besides, the structure of the impeller is also easy to manufacture, so it can be used during the pump design considering its significant effect on reducing pressure pulsation.

## 4 Conclusions

In the current paper, to reduce rotor stator interaction, the staggered impeller is designed, and the numerical simulation method is adopted to investigate its effect on pressure pulsation and performance. During calculation, twenty monitoring points are set around the impeller exit to obtain pressure pulsation signals, which are finally compared with the original impeller. The main conclusions are obtained.

The special staggered impeller contributes to the pump head increasing, which is about 3% at the design working condition. For the pump efficiency, the staggered impeller is almost identical with the original pump.

Caused by the RSI effect, the distinct peak at  $f_{BPF}$  is the predominant component in pressure spectrum. By using the staggered impeller, RSI effect will be alleviated significantly. At three calculated working conditions, the reductions are more than 80% at  $f_{BPF}$ . Meanwhile, the component at  $2f_{BPF}$  is almost unaffected. So, pressure pulsations of the model pump will be alleviated evidently by the staggered impeller.

Due to the rib in the staggered impeller, flow structures within the blade channel will be affected. Relative velocity within the front blade channel will be increased. Flow structures around the blade inlet of staggered impeller are more complex as characterized by the coherent structures. It means that the rib will affect the flow distribution within the impeller even for the low specific speed pump.

Considering its significant effect on reducing pressure pulsation, the staggered impeller can be used during the pump design. In the future, some experiments will be conducted to verify the effect. Meanwhile, the low specific speed model pump is used for investigation in the current work, so more investigations on the pumps with higher specific speeds are also imperative to validate its applicability in other pumps.

## Acknowledgments

The work is supported by the Natural Science Foundation of China No:51706086.

## Authors' contributions

Ning Zhang writes the paper. Bo Gao is in charge of the design of the pump. Xiaokai Liu carried out the numerical simulation of the model pump. Junxian Jiang conducted the data analysis.

## Competing interests

The authors declare no competing interests of the paper.

## Availability of data and materials

The data and materials of the paper can be sent by reasonable request.

## References

- [1] Y G Lu, R S Zhu, X L Wang, Y Wang, Q Fu, D X Ye. Study on the complete rotational characteristic of coolant pump in the gas-liquid two-phase operating condition. *Annals of Nuclear Energy*, 2019, 123:180-189.
- [2] D Ni, M G Yang, B Gao, N Zhang, Z Li. Numerical study on the effect of the diffuser blade trailing edge profile on flow instability in a nuclear reactor coolant pump. *Nuclear Engineering and Design*, 2017, 322:92-103.
- [3] R Barrio, J Fernandez, E Blanco, J Parrondo. Estimation of radial load in centrifugal pumps using computational fluid dynamics. *Eur. J. Mech. B/Fluids*, 2011, 30:316-324.
- [4] R Spence, J Aaral-Teixeira. A CFD parametric study of geometrical variations on the pressure pulsations and performance characteristics of a centrifugal pump. *Comput. Fluids*, 2009, 38(6):1243-1257.
- [5] Z X Gao, W R Zhu, L Lu, J Deng, J G Zhang, F J Wang. Numerical and experimental study of unsteady flow in a large centrifugal pump with stay vanes. *ASME J. Fluids Eng*, 2014, 136 (7):071101.

- [6]R Barrio, J Parrondo, E Blanco. Numerical analysis of the unsteady flow in the near-tongue region in a volute-type centrifugal Pump for different operating points. *Comput. Fluids*, 2010, 39 (5):859-870.
- [7]J F Zhang, D Appiah, F Zhang, S Q Yuan, Y D Gu, SN Asomani. Experimental and numerical investigations on pressure pulsation in a pump mode operation of a pump as turbine. *Energy Sci Eng*, 2019, 7:1264-1279.
- [8]Y Fu, J Yuan, S Yuan, G Pace, L D'Agostino, P Huang, X Li. Numerical and experimental analysis of flow phenomena in a centrifugal pump operating under low flow rates. *ASME J. Fluids Eng*, 2015, 137(1):011102.
- [9]C G Rodriguez, E Egusquiza, I F Santos. Frequencies in the vibration induced by the rotor stator interaction in a centrifugal pump turbine. *ASME J. Fluids Eng*, 2007, 129:1428-1435.
- [10]Z F Yao, F J Wang, L X Qu, R F Xiao, C L He, M Wang. Experimental investigation of time-frequency characteristics of pressure fluctuations in a double suction centrifugal pump. *ASME J. Fluids Eng*, 2011, 133 (10):101303.
- [11]Pavesi G, Cavazzini G, Ardizzon G. Time-frequency characterization of the unsteady phenomena in a centrifugal pump. *Int. J. Heat Fluid Flow*, 2008, 29(5):1527-1540.
- [12]J L Parrondo-Gayo, J Gonzalez-Perez, J Fernandez-Francos. The effect of the operating point on the pressure fluctuations at the blade passage frequency in the volute of a centrifugal pump. *ASME J. Fluids Eng*, 2002, 124(3):784-790.
- [13]S S Yang, H L Liu, F Y Kong, B Xia, L W Tan. Effects of the radial gap between impeller tips and volute tongue influencing the performance and pressure pulsations of pump as turbine. *ASME J. Fluids Eng*, 2014, 136(5): 054501.
- [14]A Posa, A Lippolis. Effect of working conditions and diffuser setting angle on pressure fluctuations within a centrifugal pump. *Int. J. Heat Fluid Flow*, 2019, 75:44-60.
- [15]A M Al-Qutub, A E Khalifa, F A Al-Sulaiman. Exploring the effect of V-Shaped cut at blade exit of a double volute centrifugal pump. *ASME Journal of Pressure Vessel Technology*, 2012, 134:021301.
- [16]J Keller, E Blanco R Barrio, J Parrondo. PIV measurements of the unsteady flow structures in a volute centrifugal pump at a high flow rate. *Exp. Fluid*, 2014, 10 (55):1820.
- [17]B Gao, N Zhang, Z Li, D Ni, M G Yang. Influence of the blade trailing edge profile on the performance and unsteady pressure pulsations in a low specific speed centrifugal pump. *ASME J. Fluids Eng*, 2016, 138(5):051106.
- [18]N Zhang, X K Liu, B Gao, X J Wang, B Xia. Effects of modifying the blade trailing edge profile on unsteady pressure pulsations and flow structures in a centrifugal pump. *Int. J. Heat Fluid Flow*, 2019, 75:227-238.
- [19]N Zhang, X Liu, B Gao, B Xia. DDES analysis of the unsteady wake flow and its evolution of a centrifugal pump. *Renewable Energy*, 2019, 141:570-582.
- [20]B Kye, K Parka, H Choia, M Lee, J Kim. Flow characteristics in a volute-type centrifugal pump using large eddy simulation. *International Journal of Heat and Fluid Flow*, 2018, 72:52-60.
- [21]N Zhang, J X Jiang, B Gao, X K Liu, D Ni. Numerical analysis of the vortical structure and its unsteady evolution of a centrifugal pump. *Renewable Energy*, 2020, 155:748-760.
- [22]J Pei, W J Wang, G Pavesi, M K Osman, F Meng. Experimental investigation of the nonlinear pressure fluctuations in a residual heat removal pump. *Annals of Nuclear Energy*, 2019, 131:63-79.
- [23]D Ni, N Zhang, B Gao, Z Li, M G Yang. Dynamic measurements on unsteady pressure pulsations and flow distributions in a nuclear reactor coolant pump. *Energy*, 2020, 198:117305.
- [24]A Posa, A Lippolis, E Balaras. Investigation of separation phenomena in a radial pump at reduced flow rate by large-eddy simulation. *ASME J. Fluids Eng*, 2016, 138 (12):121101.
- [25]N Zhang, J X Jiang, B Gao, X K Liu. DDES analysis of unsteady flow evolution and pressure pulsation at off-design condition of a centrifugal pump. *Renewable Energy*, 2020, 153:193-204.
- [26]A Posa, A Lippolis, R Verzicco, E Balaras. Large-Eddy simulations in mixed-flow pumps using an immersed-boundary method. *Comput. Fluids*, 2011, 47 (1):33-43.
- [27]W Jiang, G J Li, P F Liu, L Fu. Numerical investigation of influence of the clocking effect on the unsteady pressure fluctuations and radial forces in the centrifugal pump with vaned diffuser. *Int. Commun. Heat Mass Tran*, 2016, 71:164-171.
- [28]D Zhang, W Shi, B Bart van Esch, L Shi, M Dubuisson. Numerical and experimental investigation of tip leakage vortex trajectory and dynamics in an axial flow pump. *Comput. Fluids*, 2015, 112:61-71.
- [29]N Zhang, B Gao, D Ni, X K Liu. Coherence analysis to detect unsteady rotating stall phenomenon based on pressure pulsation signals of a centrifugal pump. *Mechanical Systems and Signal Processing*, 2021, 148:107161.
- [30]N Zhang, F K Zheng, X K Liu, B Gao, G P Li. Unsteady flow fluctuations in a centrifugal pump measured by laser Doppler anemometry and pressure pulsation. *Phys. Fluids*, 2020, 32:125108.
- [31]D Z Wu, P Yan, X Chen, P Wu, S Yang. Effect of trailing-edge modification of a mixed-flow pump. *ASME J. Fluids Eng*, 2015, 138:101205.
- [32]K Wang, Z X Zhang, L L Jiang, H L Liu, Y Li. Effects of impeller trim on performance of two-stage self-priming centrifugal pump. *Adv Mech Eng*, 2017, 9(2):1-11.
- [33]W J Wang, J Pei, S Q Yuan, T Y Yin. Experimental investigation on clocking effect of vaned diffuser on performance characteristics and pressure pulsations in a centrifugal pump. *Experimental Thermal and Fluid Science*, 2018, 90: 286-298.
- [34]Q Q Li, S Y Li, P Wu, B Huang, D Z Wu. Investigation on reduction of pressure fluctuation for a double-suction centrifugal pump. *Chinese Journal of Mechanical Engineering*, 2021, 34(12):1-18.

- [35]Y Tao, S Q Yuan, J R Liu, F Zhang. Influence of Cross-Sectional Flow Area of Annular Volute Casing on Transient Characteristics of Ceramic Centrifugal Pump. *Chinese Journal of Mechanical Engineering*, 2019, 32(4):1-13.
- [36]Y B. Liu, L Tan. Spatial-temporal evolution of tip leakage vortex in a mixed-flow pump with tip clearance. *ASME J Fluids Eng*, 2019, 141:081302.
- [37]Y B Liu, L Tan. Tip clearance on pressure fluctuation intensity and vortex characteristic of a mixed flow pump as turbine at pump mode. *Renew Energy*, 2018, 129:606-615.
- [38]A Posa, A Lippolis. A LES investigation of off-design performance of a centrifugal pump with variable-geometry diffuser. *Int. J. Heat Fluid Flow*, 2018, 70: 299314.
- [39]N Zhang, B Gao, Z Li, D Ni, Q Jiang. Unsteady flow structure and its evolution in a low specific speed centrifugal pump measured by PIV. *Exp. Therm. Fluid Sci*, 2018, 97:133-144.

# Figures

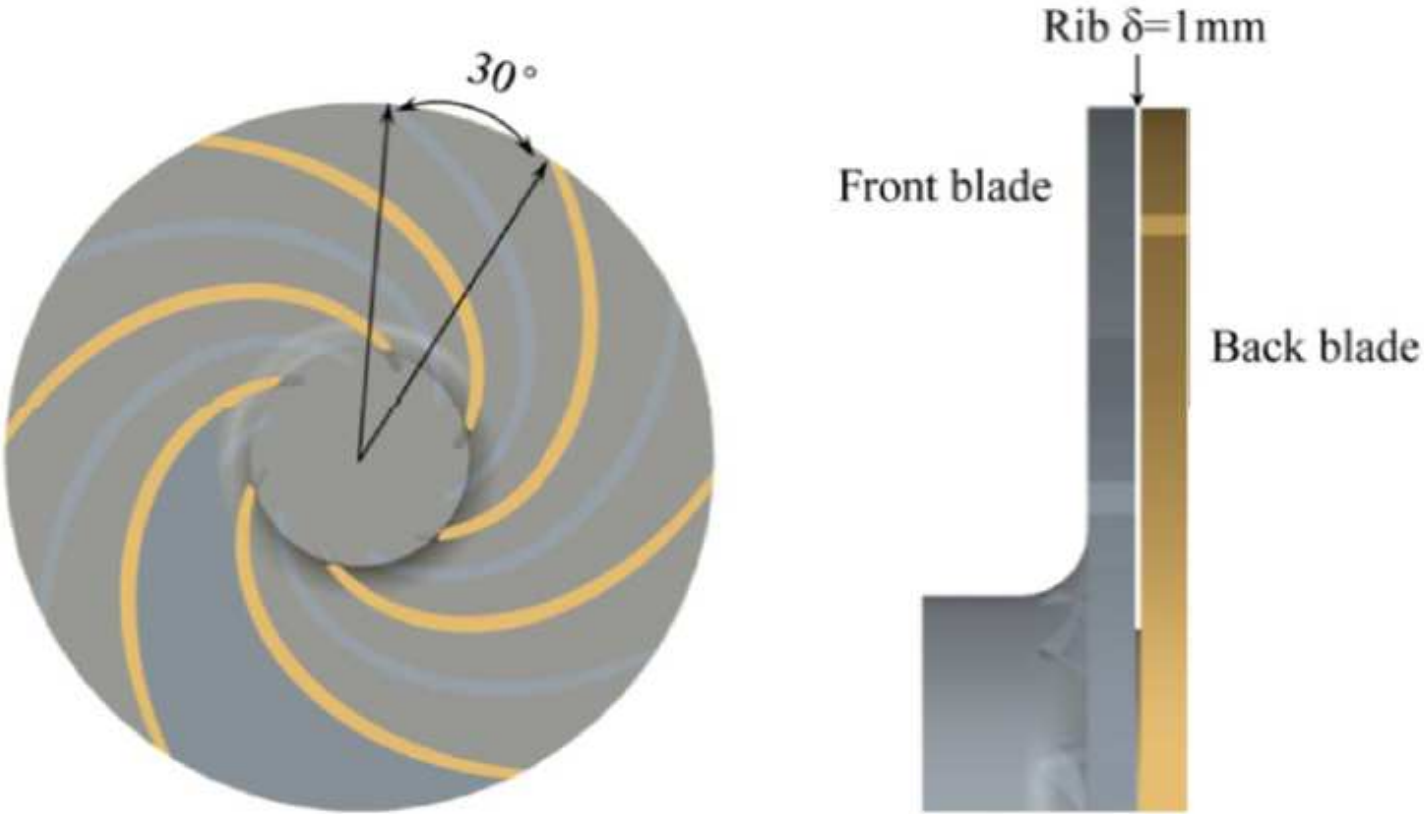


Figure 1

Structure of the staggered impeller

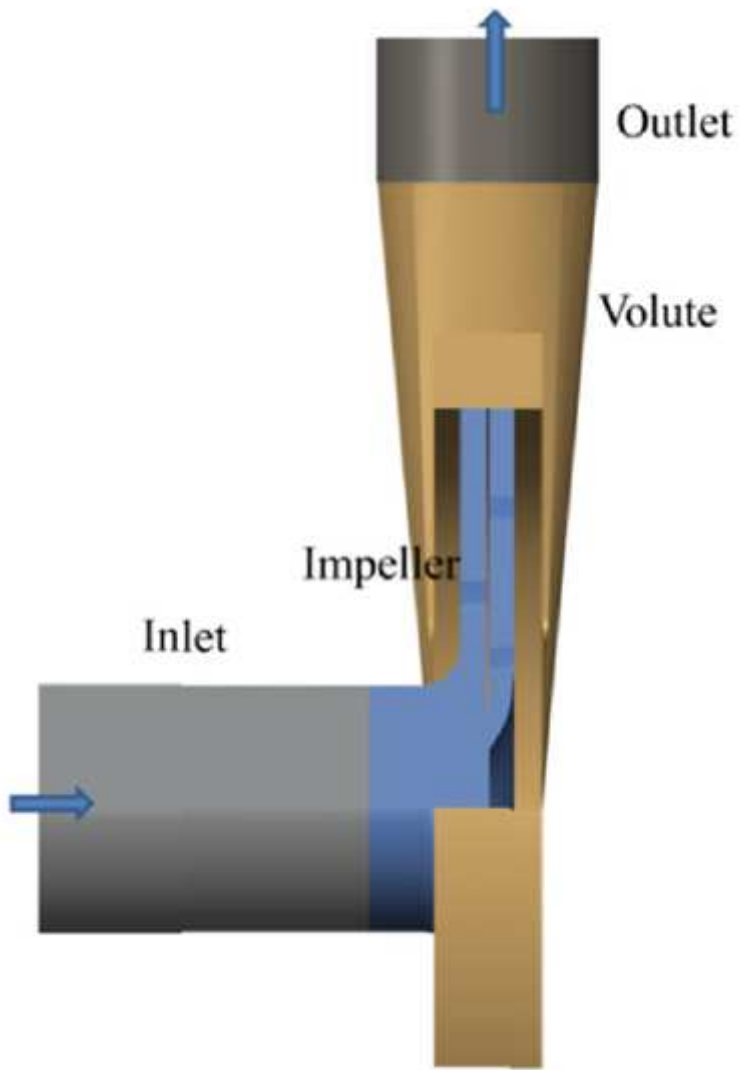


Figure 2

Computational domain established for calculation

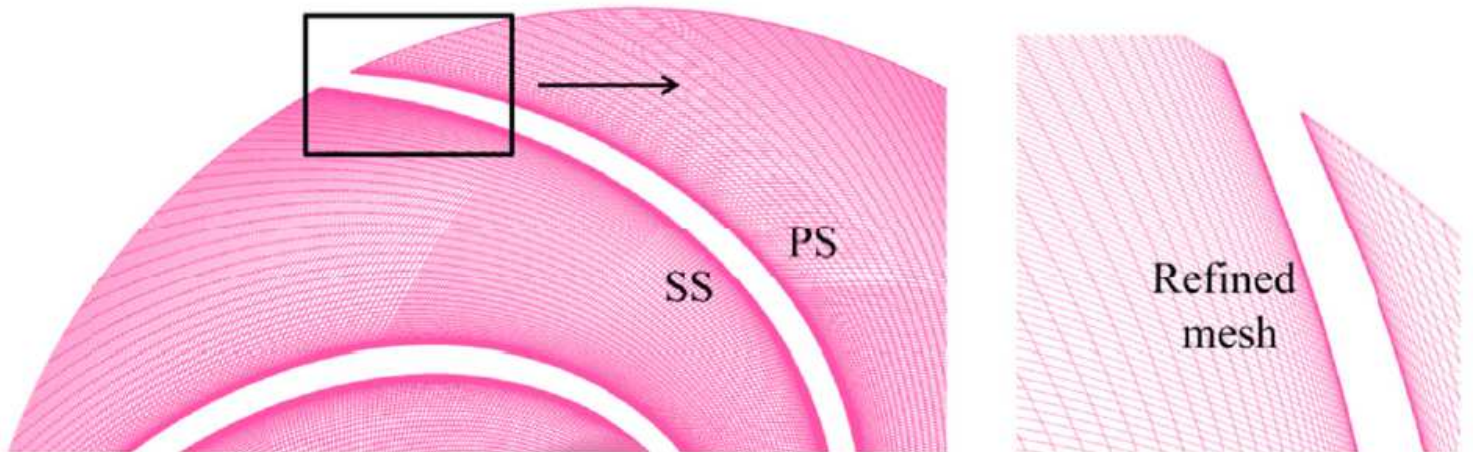


Figure 3

Mesh grids of the used staggered blade

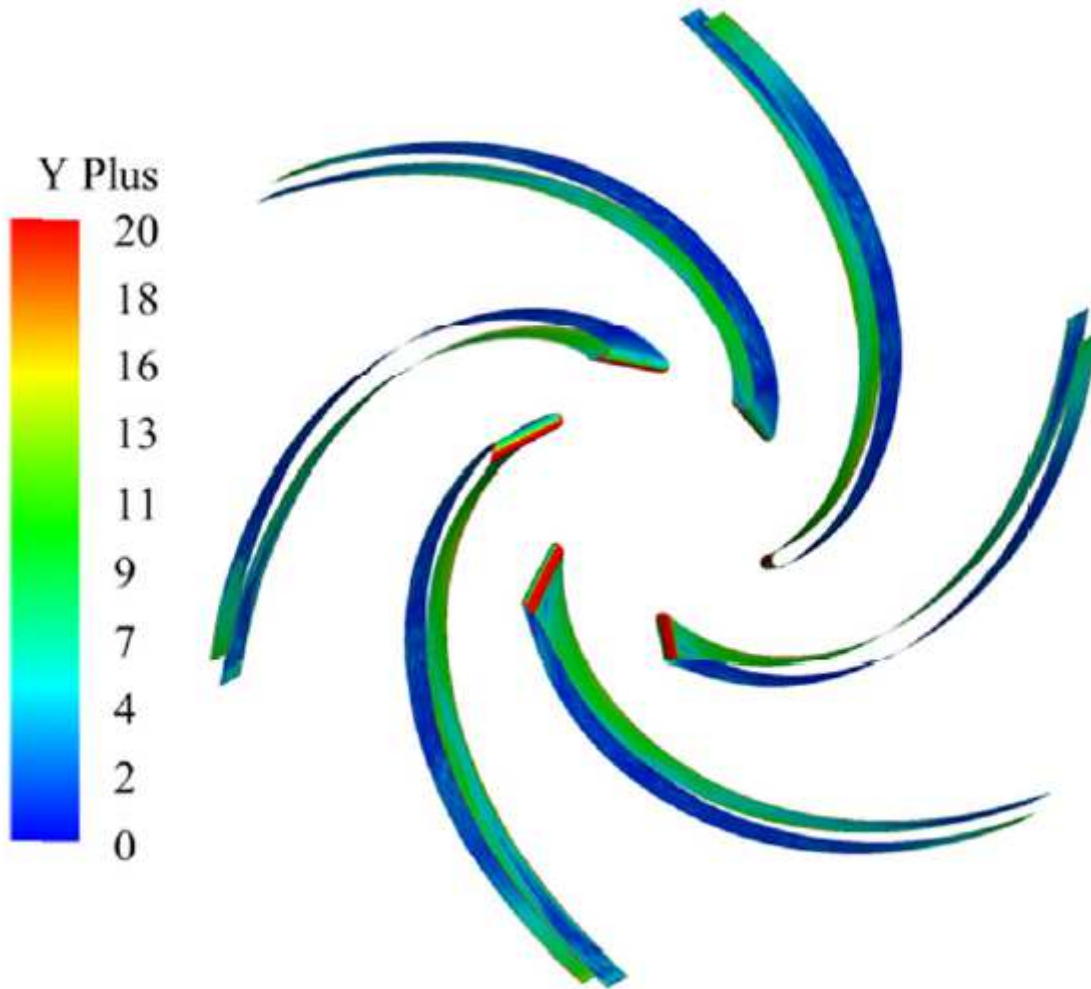


Figure 4

Values of  $y^+$  on the blade surface at the design flow rate

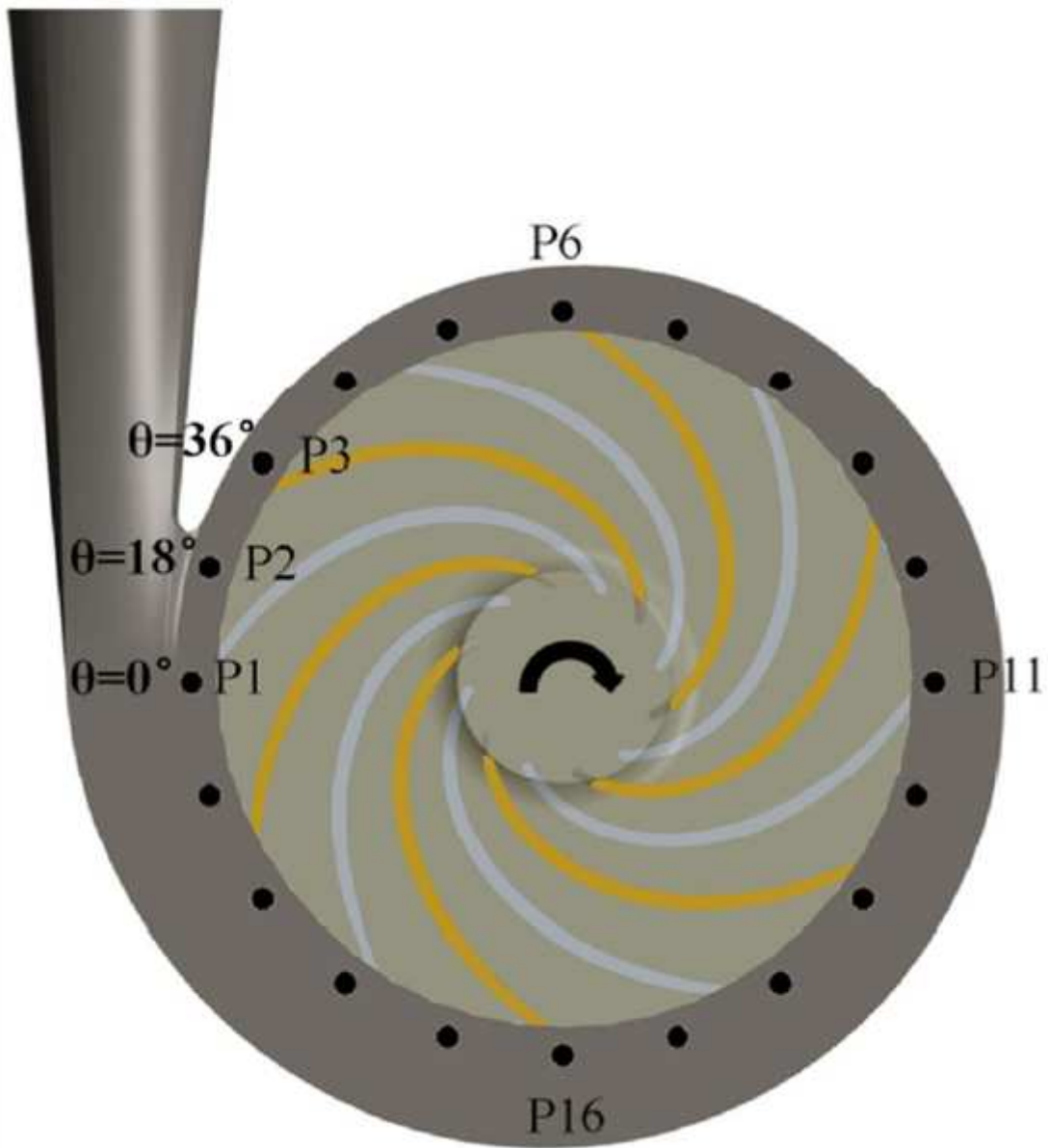


Figure 5

Twenty points around the impeller exit during calculation

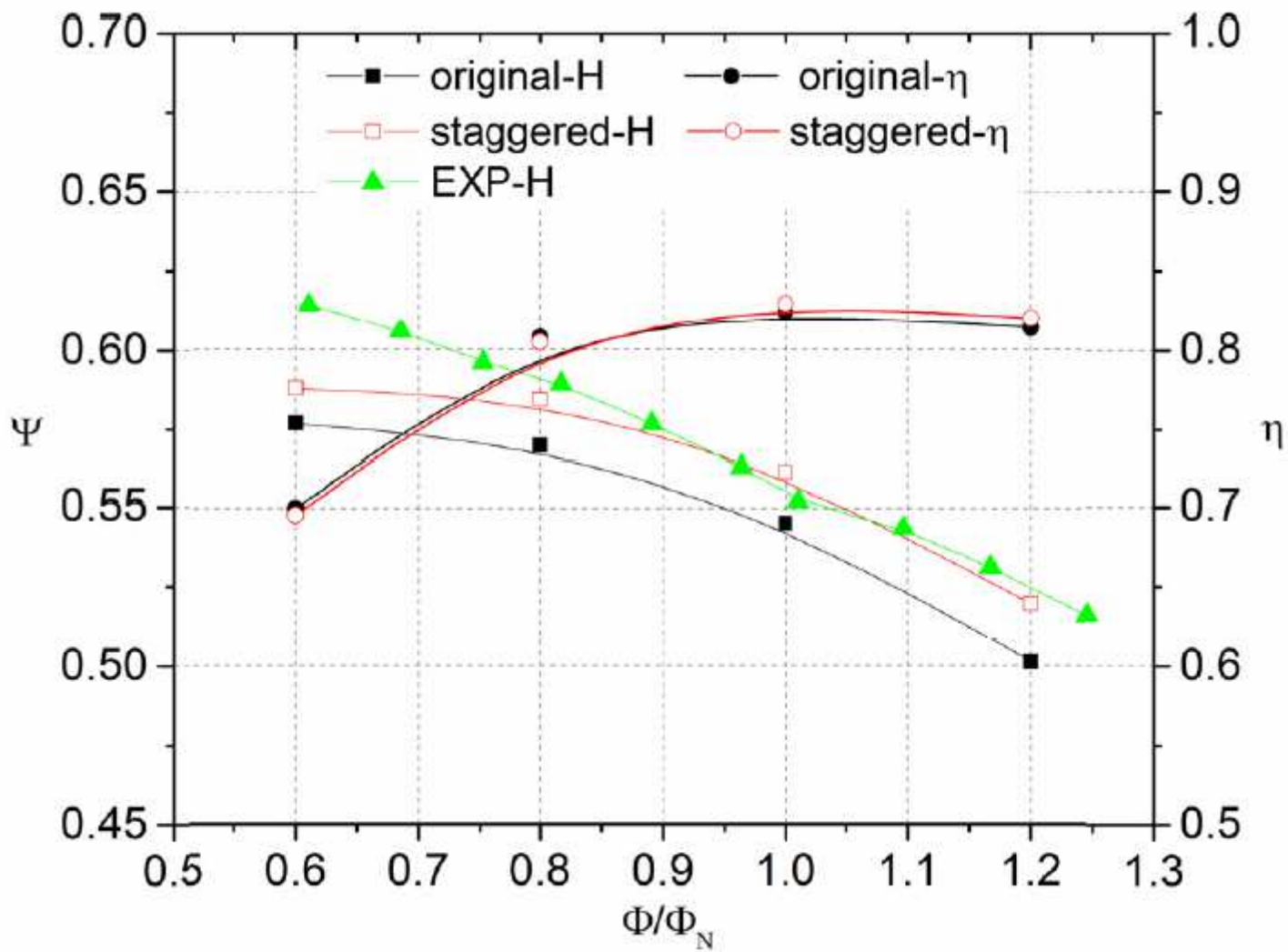


Figure 6

Pump performance comparison

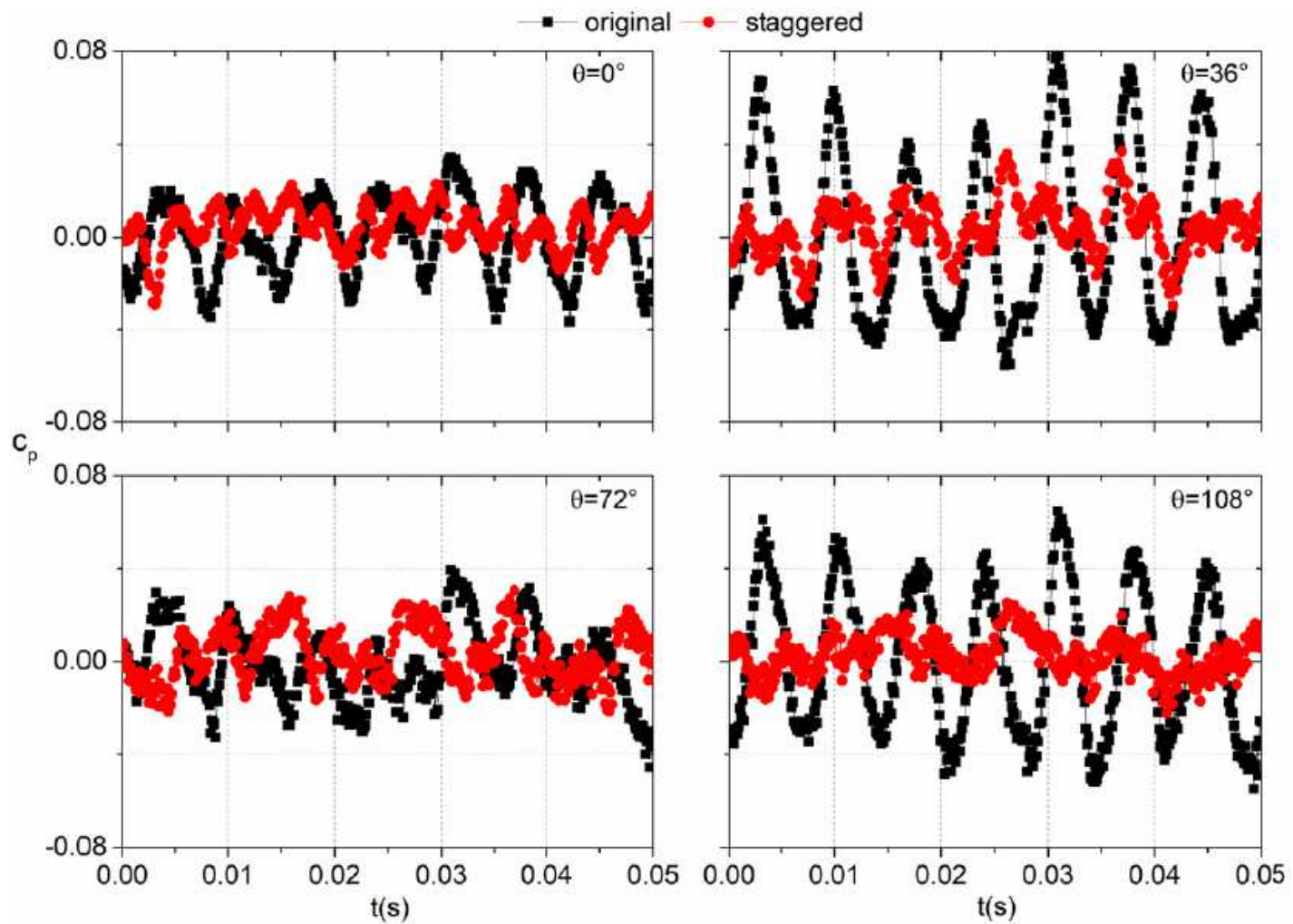


Figure 7

Pressure signals at four points of the original and staggered impellers

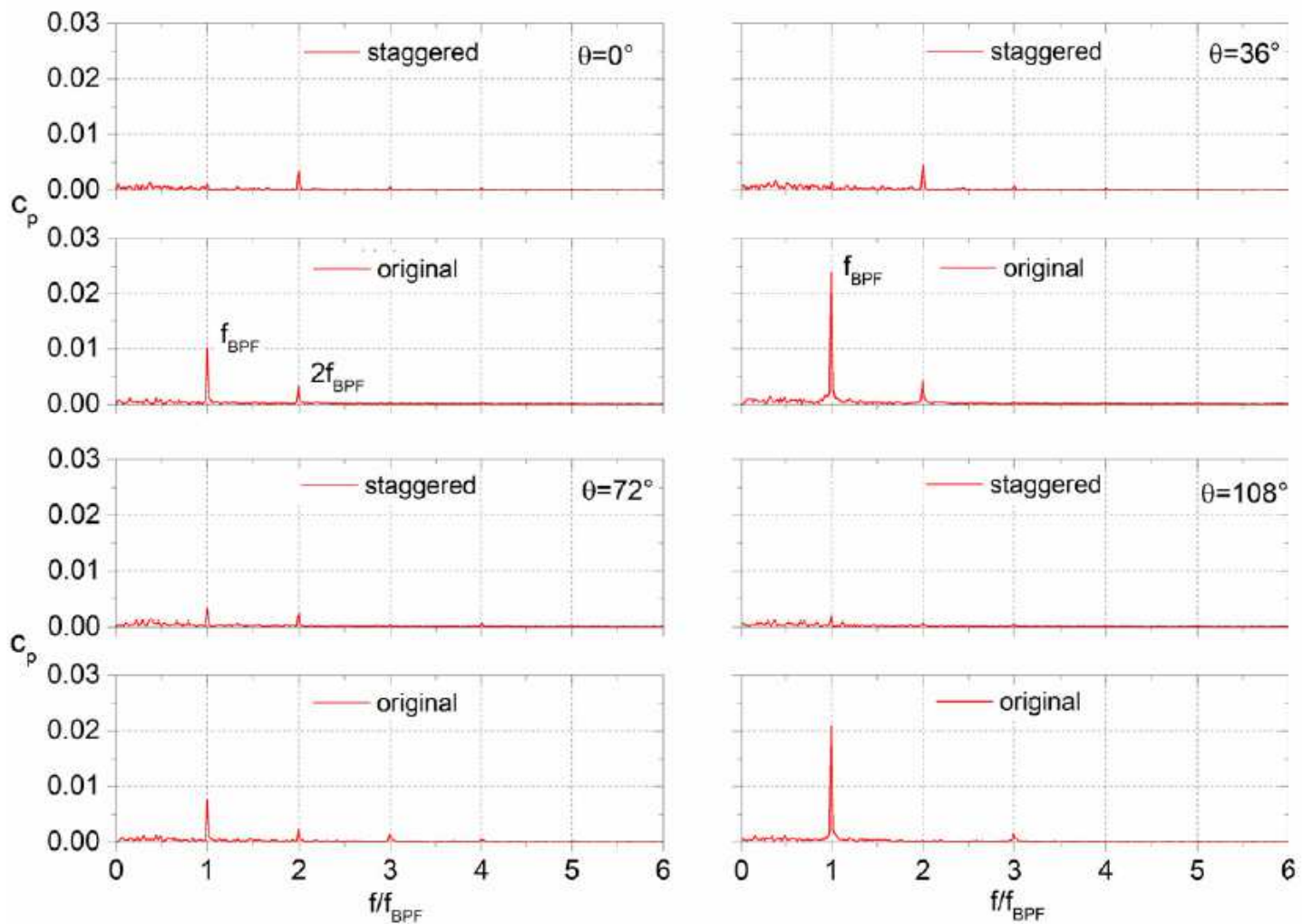


Figure 8

Pressure spectra at four points from  $\theta=0^\circ$  to  $\theta=108^\circ$  of the original and staggered impellers

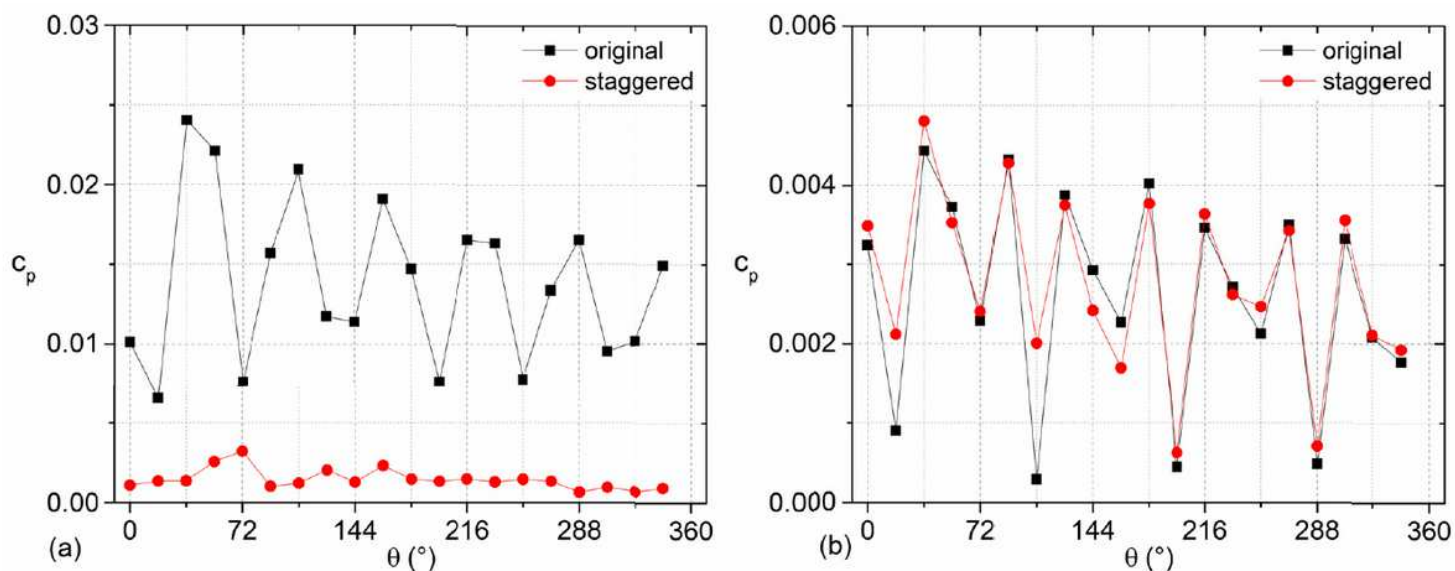


Figure 9

Pressure amplitudes at twenty points under the design working condition, (a)fBPF, (b)2fBPF

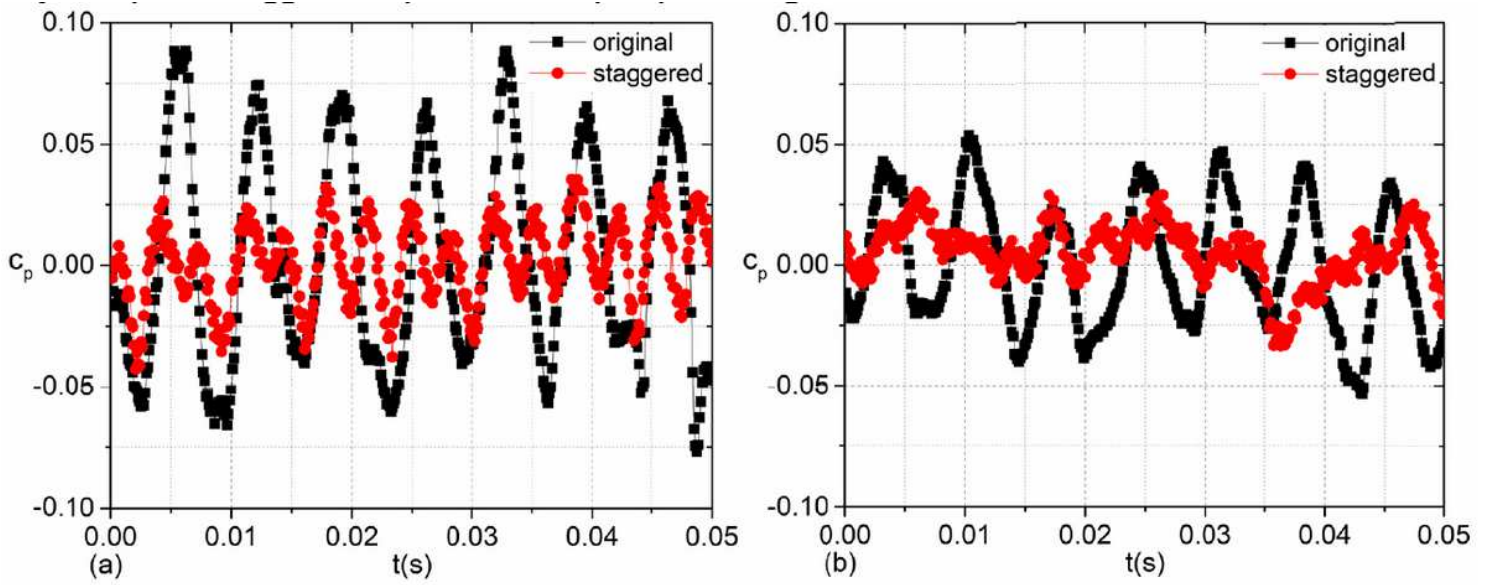


Figure 10

Comparison of pressure signals at  $\theta=36^\circ$ , (a)1.2 $\Phi$ N, (b)0.8 $\Phi$ N

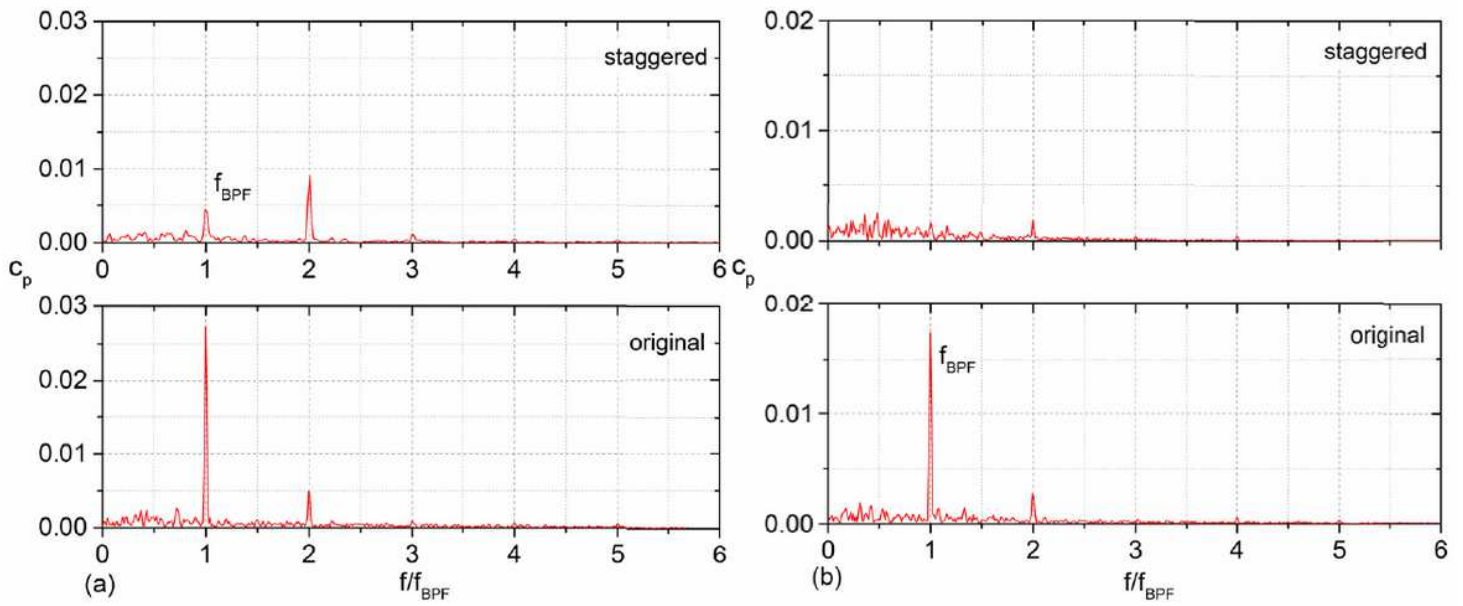


Figure 11

Pressure spectra at  $\theta=36^\circ$  of the staggered and original impellers, (a)1.2 $\Phi$ N, (b)0.8 $\Phi$ N

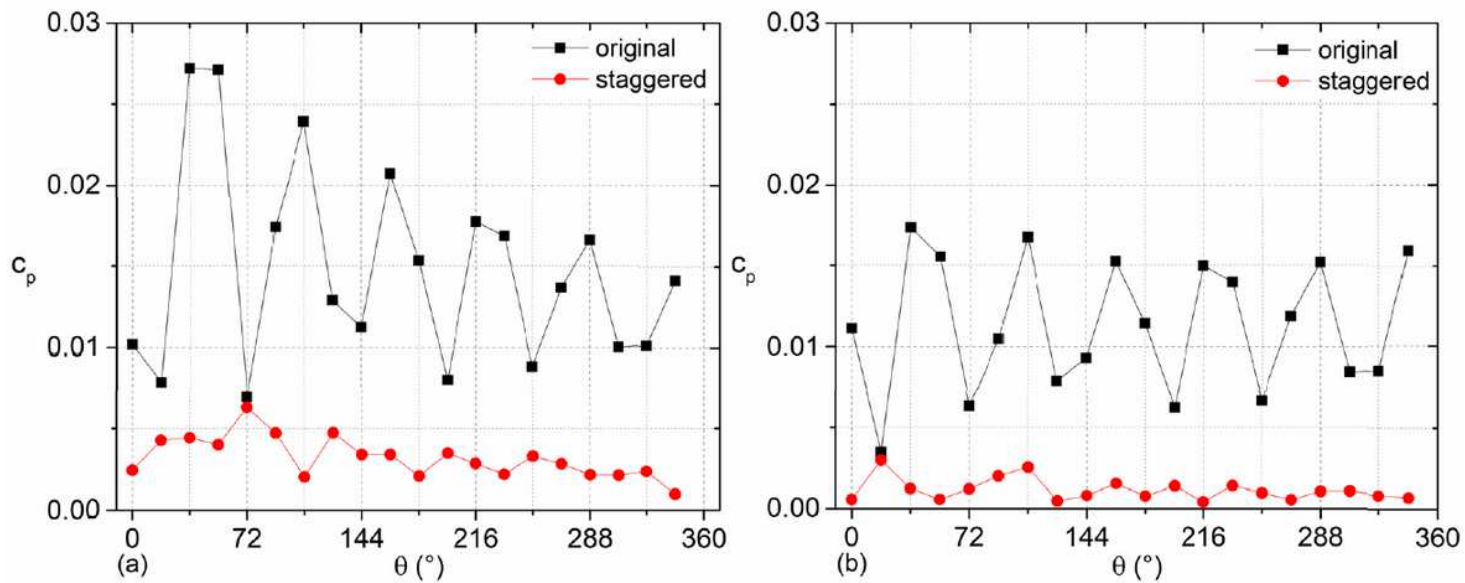


Figure 12

Pressure amplitudes of the twenty points at fBPF, (a)  $1.2\Phi_N$ , (b)  $0.8\Phi_N$

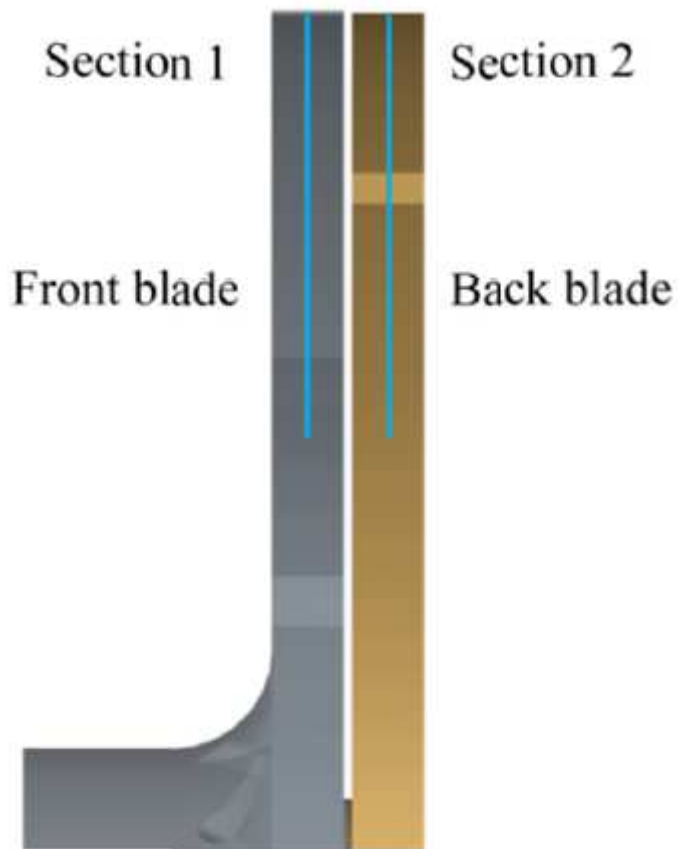


Figure 13

Two cut planes selected for investigation

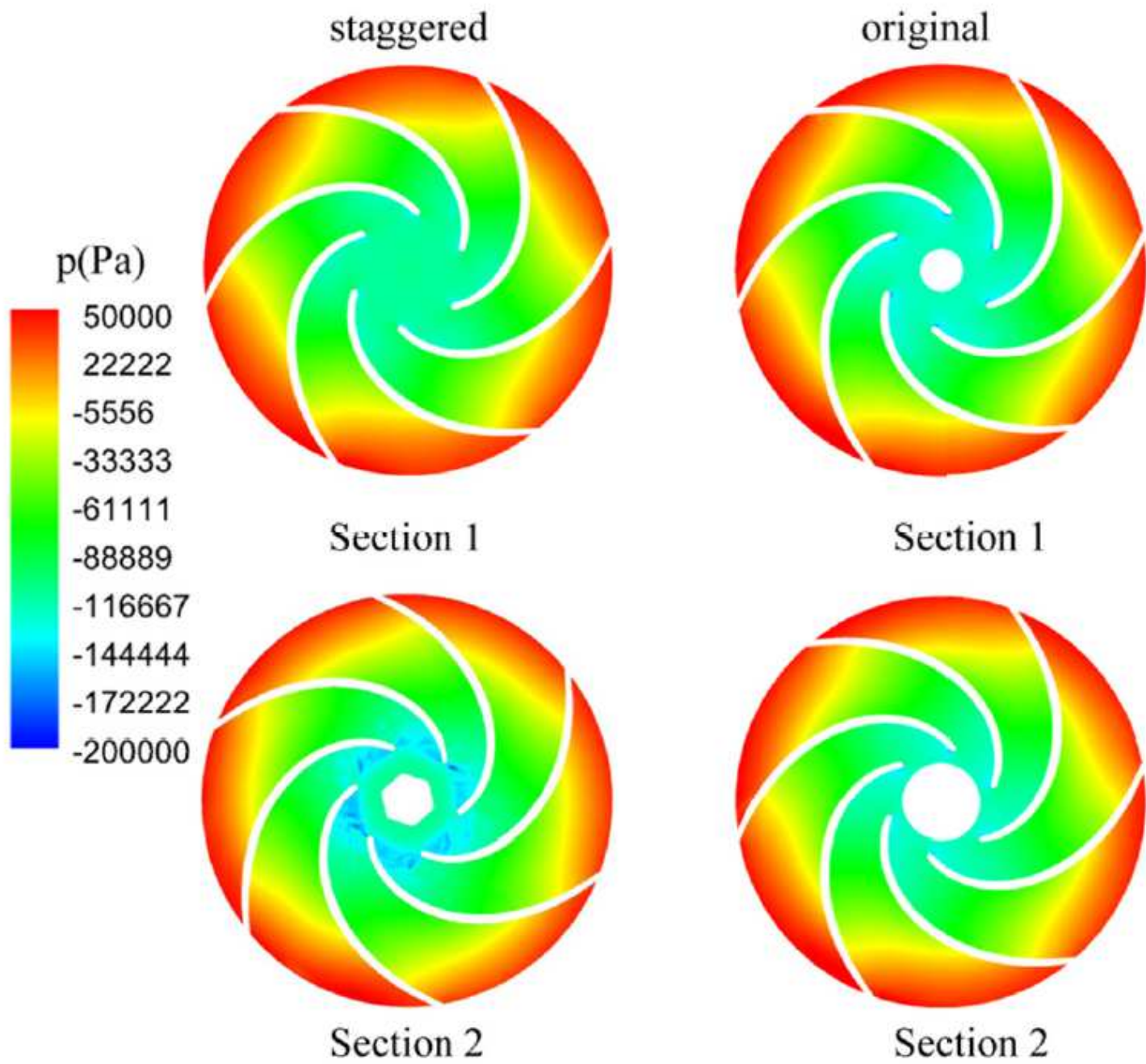


Figure 14

Static pressure distributions on Section1 and Section2

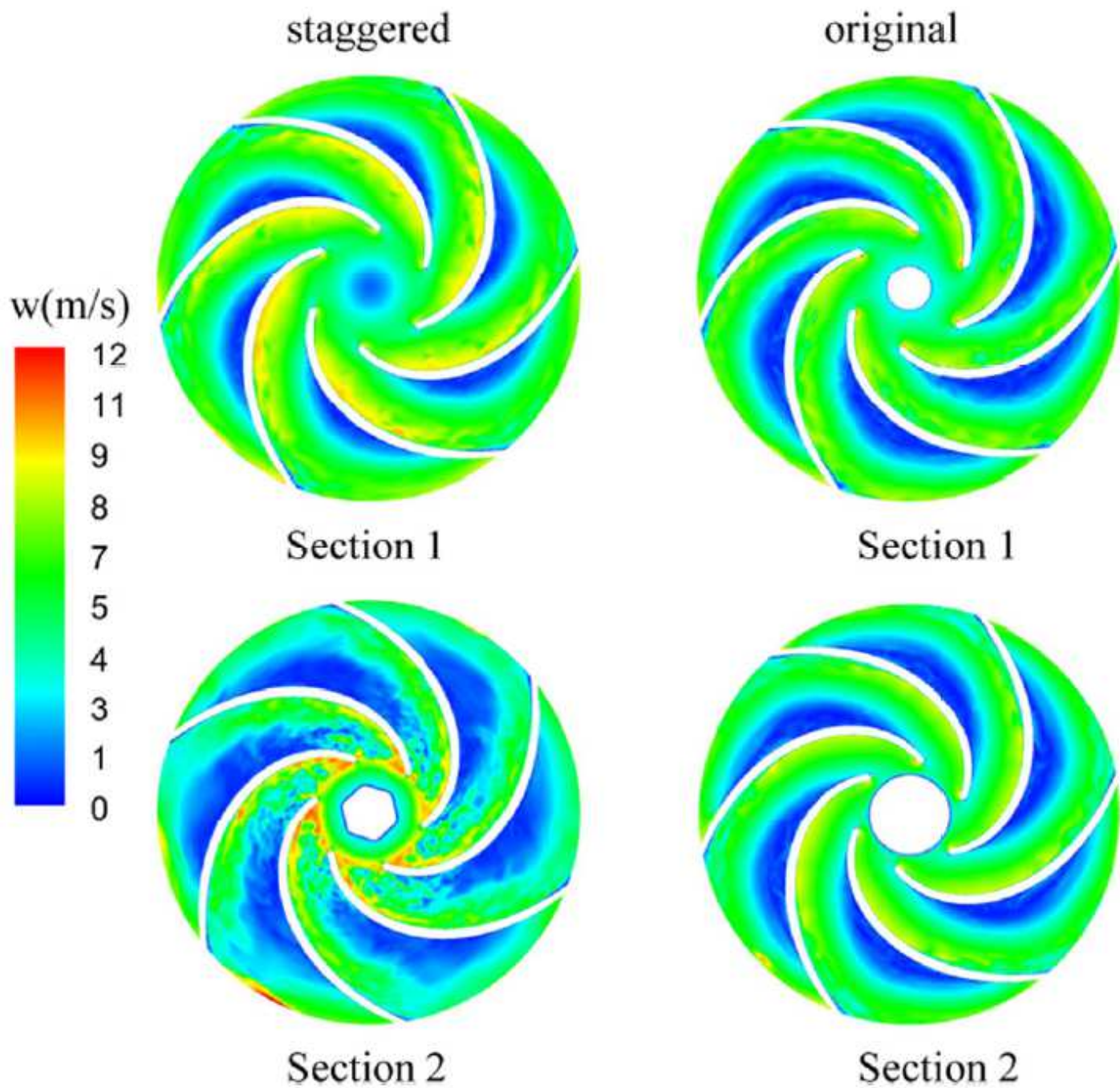


Figure 15

Relative velocity distributions on Section1 and Section2

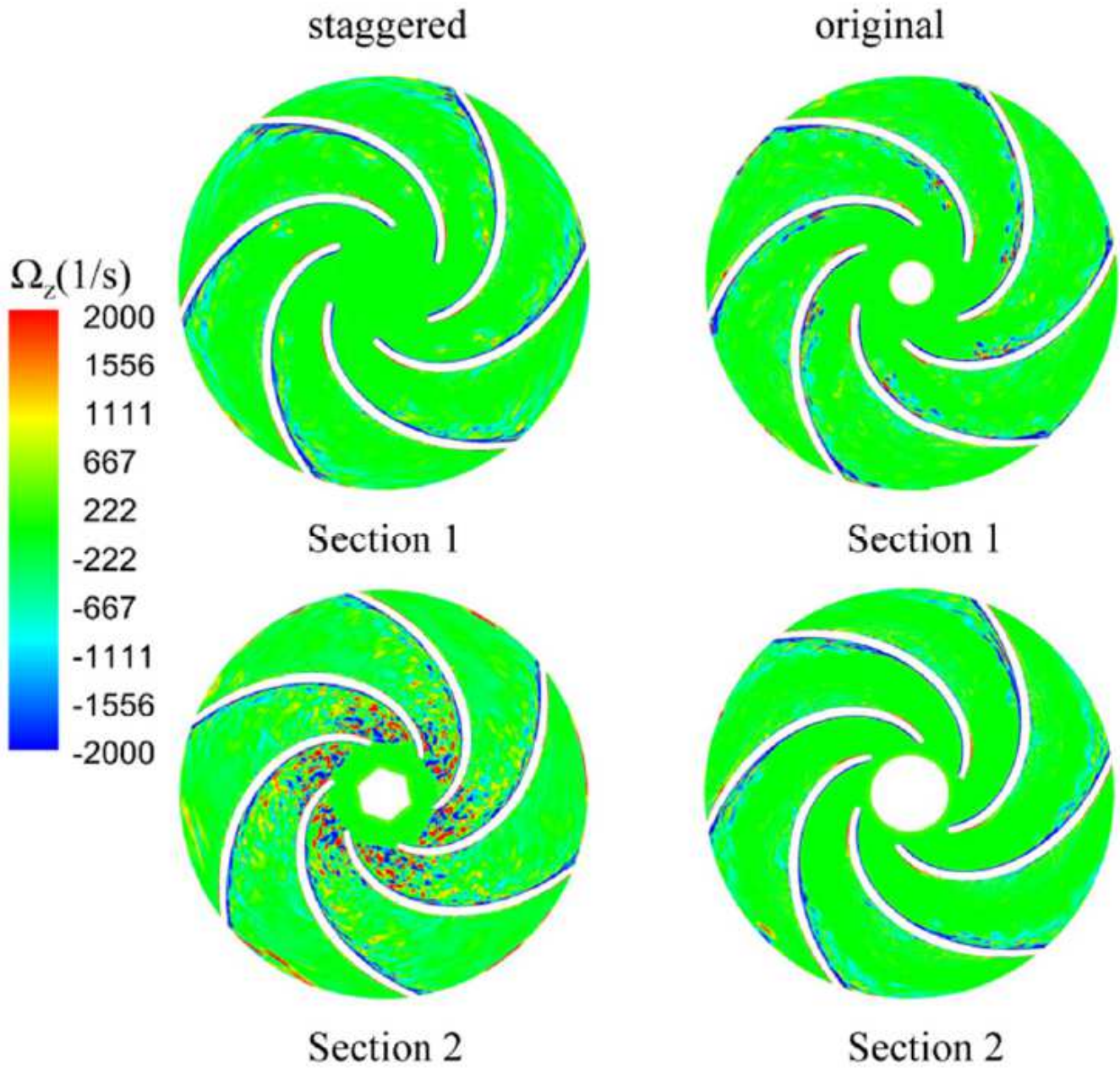


Figure 16

Vorticity distributions on Section1 and Section2 of the two impellers